Electronic Supplementary Information

Cobalt, nickel, and iron complexes of 8-hydroxyquinoline-di(2-picolyl)amine for light-driven hydrogen evolution

Nadia Alessandra Carmos dos Santos,[a] Mirco Natali,*[b] Elena Badetti,[a] Klaus Wurst,[c] Giulia Licini[a] and Cristiano Zonta*[a]

[a] Department of Chemical Sciences, University of Padova, Via F. Marzolo 1, 35131 Padova, Italy.

E-mail: cristiano.zonta@unipd.it

[b] Department of Chemical and Pharmaceutical Sciences, University of Ferrara, and Centro Interuniversitario per la Conversione Chimica dell'Energia Solare (SolarChem), sez. di Ferrara, via L. Borsari 46, 44121 Ferrara, Italy.

E-mail: mirco.natali@unife.it

[c] Institut für Allgemeine, Anorganische und Theoretische Chemie, Innrain 80/82, A-6020 Innsbruck, Austria.

Synthesis and characterization of $Ir(ppy)_2(bpy)PF_6$

(i) Synthesis of $[Ir(ppy)_2Cl]_2$ dimer

0.5 g (1.6 mmol) $IrCl_3 \cdot xH_2O$ were dissolved in 66 mL of a 3/1 ethylene glycol monomethylether/water mixture and 0.49 mL (3.5 mmol) 2-phenylpyridine were added. The solution was heated at reflux under continuous stirring in a nitrogen atmosphere for 24 h. After that, the mixture was cooled to room temperature and 200 mL water were added to allow precipitation of the $[Ir(ppy)_2Cl]_2$ dimer. After filtration, the solid obtained was recrystallized from a 50/50 CH_2Cl_2/hexane mixture (reaction yield = 92%).

(ii) Synthesis of $Ir(ppy)_2(bpy)PF_6$

0.3 g (0.28 mmol) $[Ir(ppy)_2Cl]_2$ dimer were dissolved in 100 mL of a 50/50 CH_2Cl_2/methanol mixture and 0.09 g (0.57 mmol) 2,2'-bipyridine were added. The solution was heated at reflux under inert atmosphere for 6 h. After that, the solution was concentrated under vacuum and ca 200 mL water were added until the solution became transparent. An aliquot of concentrated KPF_6 aqueous solution was then added to favor precipitation of the desired complex. The yellow solid was filtered and recrystallized from a 50/50 CH_2Cl_2/ether mixture (reaction yield = 85%).

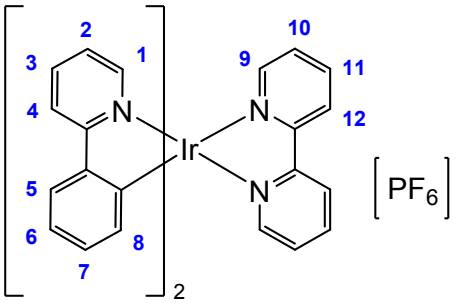

^{1}H-NMR (400 MHz, d_6-acetone, δ/ppm): 8.87 (H_9, 2H, d), 8.32 (H_{10}, 2H, t), 8.26 (H_1, 2H, d), 8.13 (H_{12}, 2H, d), 7.98 (H_2, 2H, t), 7.91 (H_5, 2H, d), 7.85 (H_4, 2H, d), 7.73 (H_{11}, 2H, t), 7.17 (H_3, 2H, t), 7.05 (H_6, 2H, t), 6.93 (H_7, 2H, t), 6.37(H_8, 2H, d).

Characterization of the hydroxiquinolinic ligand

8-hydroxyquinoline-2-carbaldehyde (1):

The final product is a yellow solid and the yield was 65%.

^{1}H NMR (200 MHz, $CDCl_3$): δ (ppm) = 10.26 (s, 1H, CHO), 8.36 (d, 1H, HAr), 8.21 (s, 1H, OH), 8.09 (d, 1H, HAr), 7.67 (t, 1H, HAr), 7.48 (dd, 1H, HAr), 7.34 (dd, 1H, HAr).

^{13}C NMR (62 MHz, $CDCl_3$): δ (ppm) = 192.94, 153.24, 150.42, 138.04, 137.72, 131.17, 130.88, 130.66, 118.26, 111.43.

ESI-MS: m/z Calc: 173.1 **Found** $[MH]^+$ m/z: 174.0.

^{1}H NMR (200 MHz, $CDCl_3$):

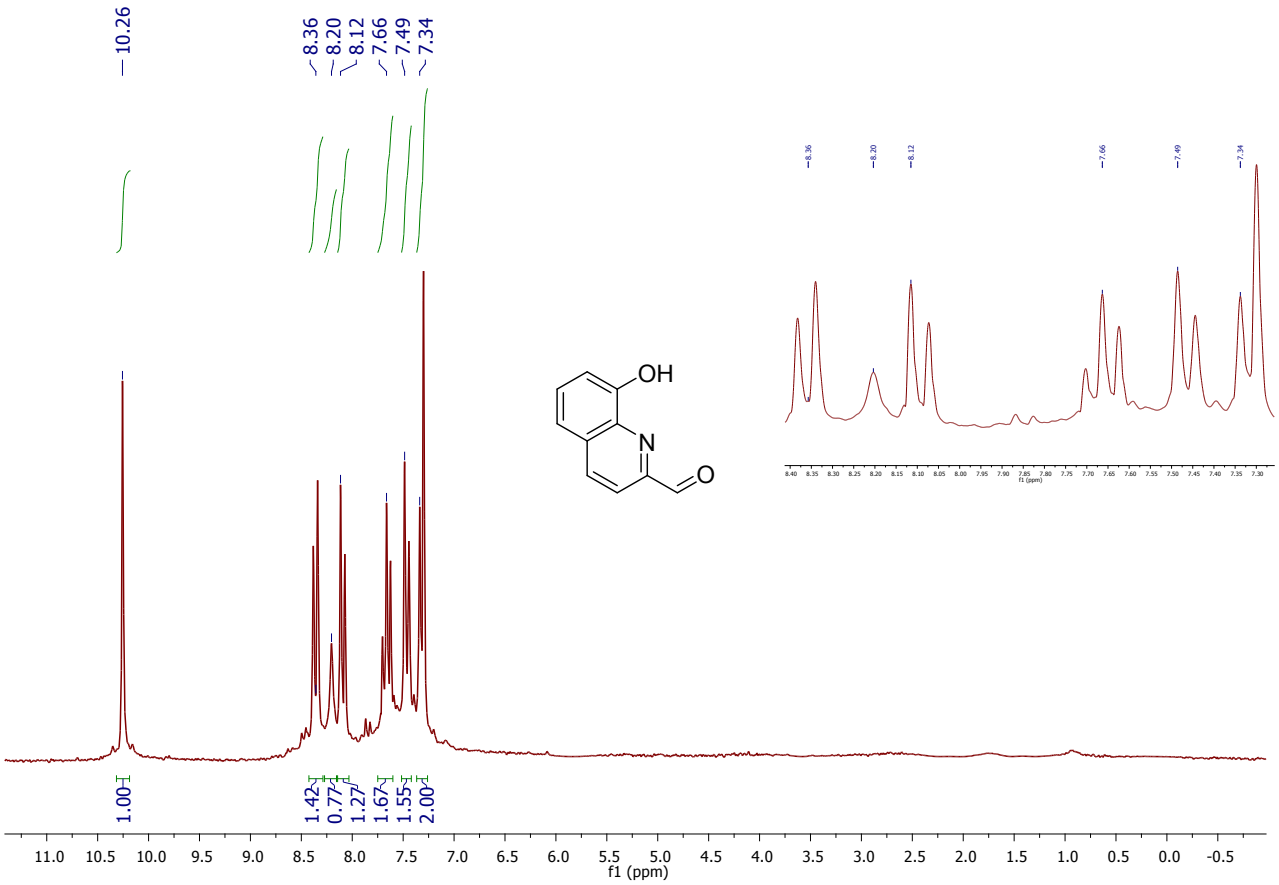

^{13}C NMR (62 MHz, $CDCl_3$):

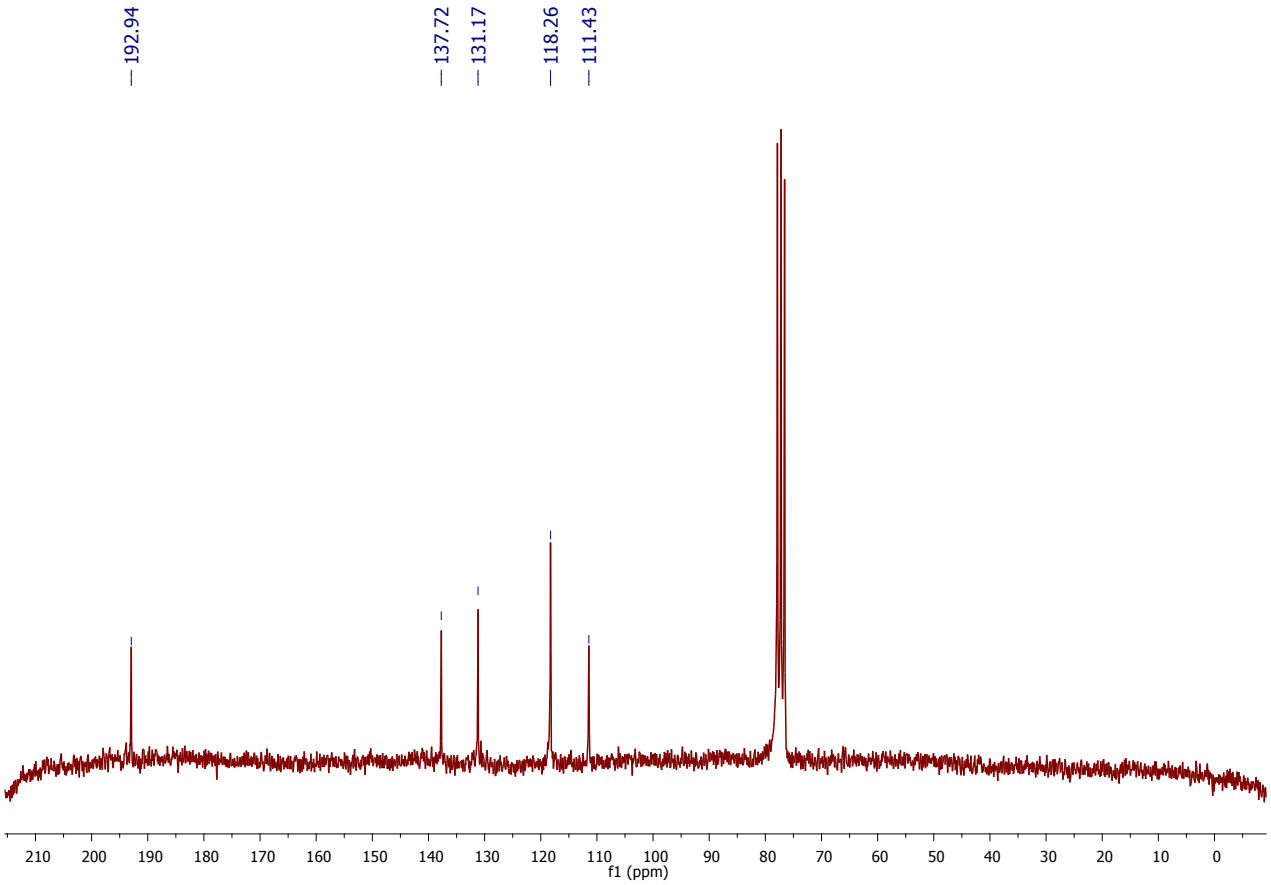

ESI+ MS (m/z):

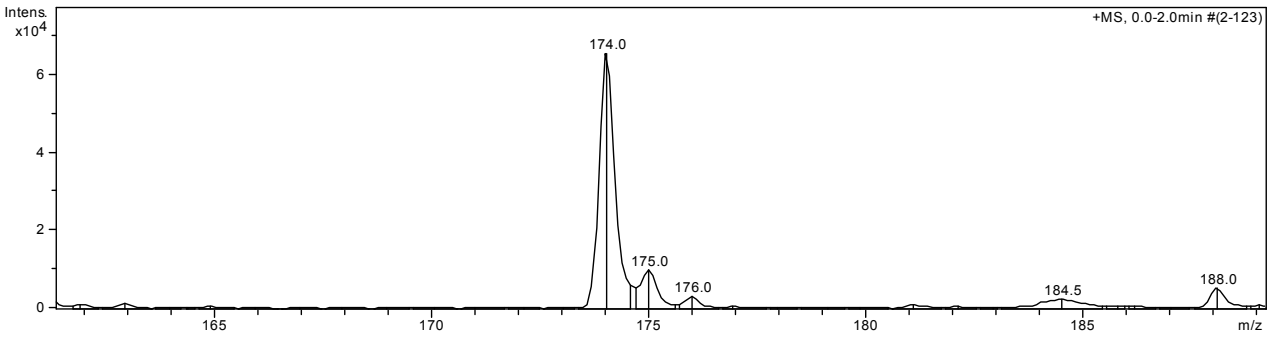

2-((bis(pyridin-2-ylmethyl)amino)methyl)quinolin-8-ol (2):

The final product is a light yellow oil and the yield was 98%.

^{1}H NMR (200 MHz, CD_3CN): δ (ppm) = 8.54 (dq, 2H, HAr), 8.24 (d, 1H, HAr), 7.70 (m, 5H, HAr), 7.43 (m, 2H, HAr), 7.18 (m, 3H, HAr), 4.03 (s, 2H, CH_2), 3.93 (s, 4H, CH_2).

^{13}C NMR (62 MHz, $CDCl_3$): δ (ppm) = 160.71, 158.62, 153.88, 150.63, 139.07, 138.01, 137.92, 128.93, 128.90, 124.74, 123.60, 123.32, 118.92, 111.56, 61.72, 61.17.

ESI-MS: m/z Calc: 356.4 **Found** $[MH]^+$ m/z: 357.4.

^{1}H NMR (200 MHz, CD_3CN):

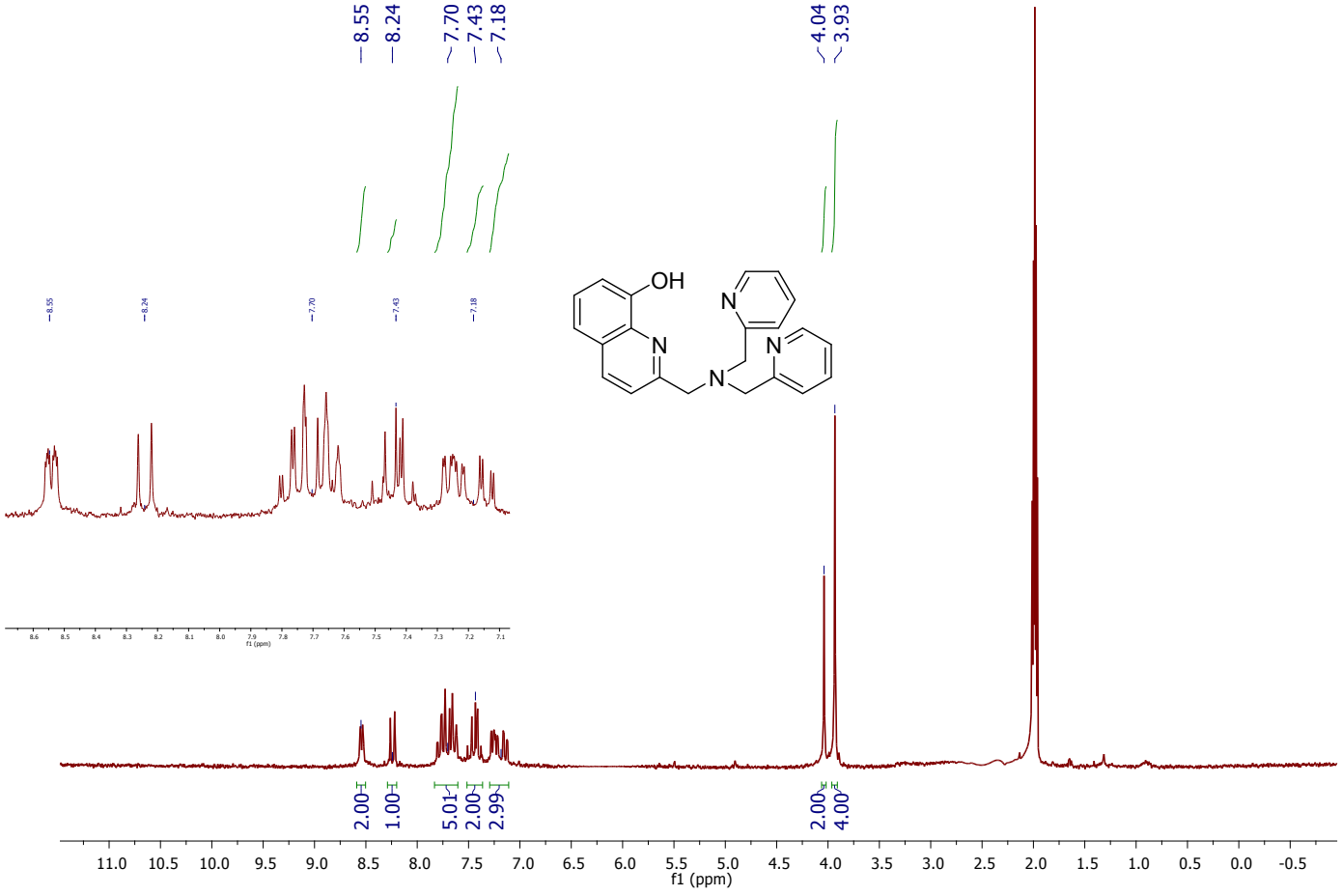

^{13}C NMR (62 MHz, $CDCl_3$):

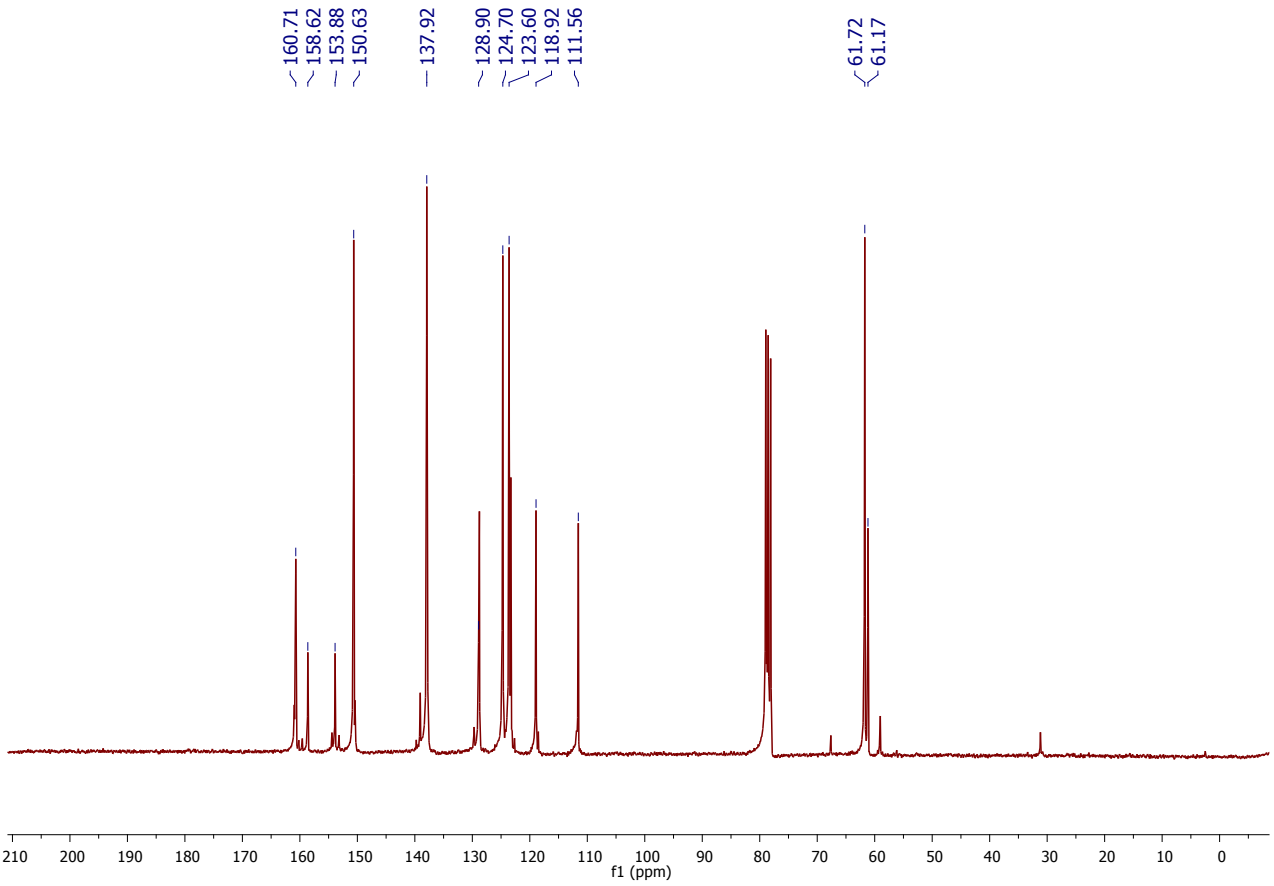

ESI+ MS (m/z):

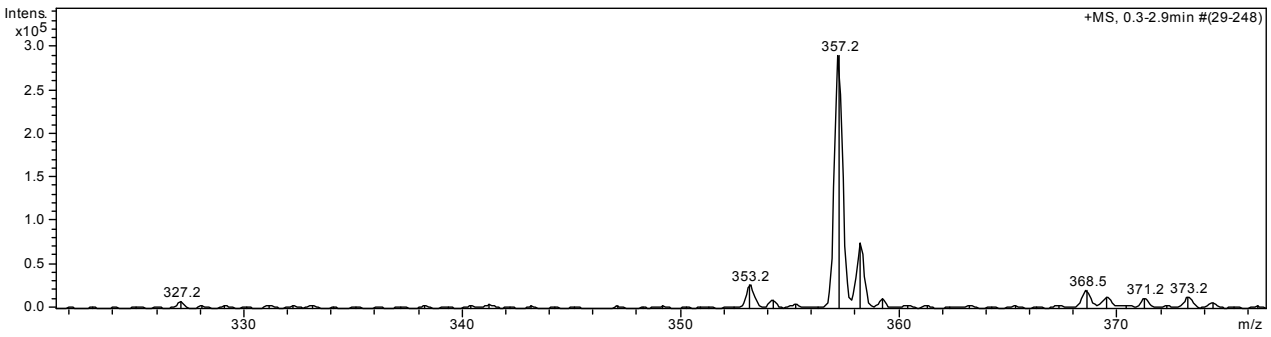

Characterization of hydroxiquinolinic complexes

Complex 3a: The final product is a dark brown crystal and the yield was 88%.

IR (KBr, cm^{-1}): 3397, 1600, 1458, 1104, 766, 628.

ESI+ MS (m/z): Calc. for $M^+ = C_{22}H_{19}CoN_4OClO_4$: 513.0, **Found** 512.9.

Elemental Analysis (calc.) $C_{22}H_{19}CoN_4O{*}2ClO_4{*}3H_2O{*}CH_3CN$ = C: 40.70%; H: 3.98%; N: 9.89% **Found** = C: 40.64%; H: 3.99%; N: 9.27%.

IR (KBr, cm^{-1})

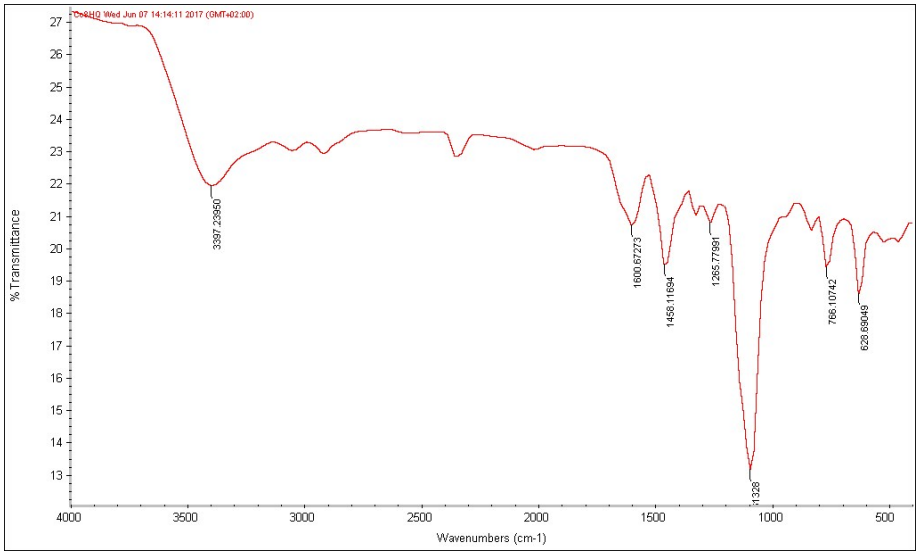

ESI+ MS (m/z)

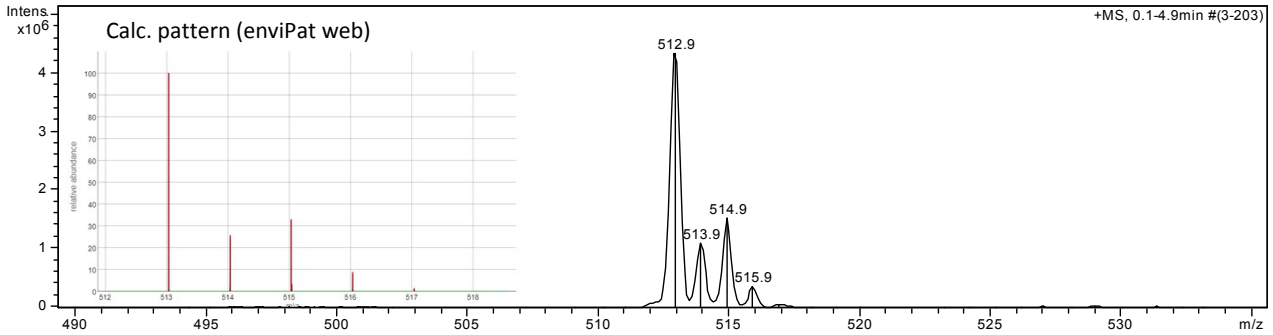

Complex 3b: The final product is an ochre crystal and the yield was 83%.

IR (KBr, cm^{-1}): 3412, 1605, 1440, 1094, 763, 627.

ESI+ MS (m/z): Calc. for M^{+} = $C_{22}H_{19}NiN_4O$: 413.1, **Found** 413.1.

ESI+ MS (m/z): Calc. for M^{2+} = $C_{22}H_{20}NiN_4O$: 207.0, **Found** 207.0.

Elemental Analysis (calc.) $C_{22}H_{19}NiN_4O*ClO_4*2H_2O$= C: 48.08%; H: 4.22%; N: 10.19% **Found** = C: 48.43%; H: 3.86%; N: 9.77%.

IR (KBr, cm^{-1})

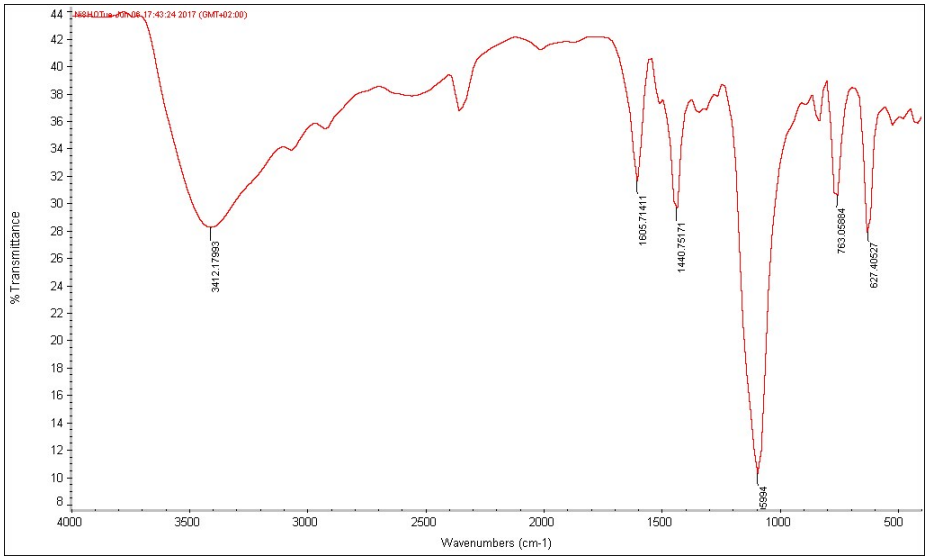

ESI+ MS (m/z)

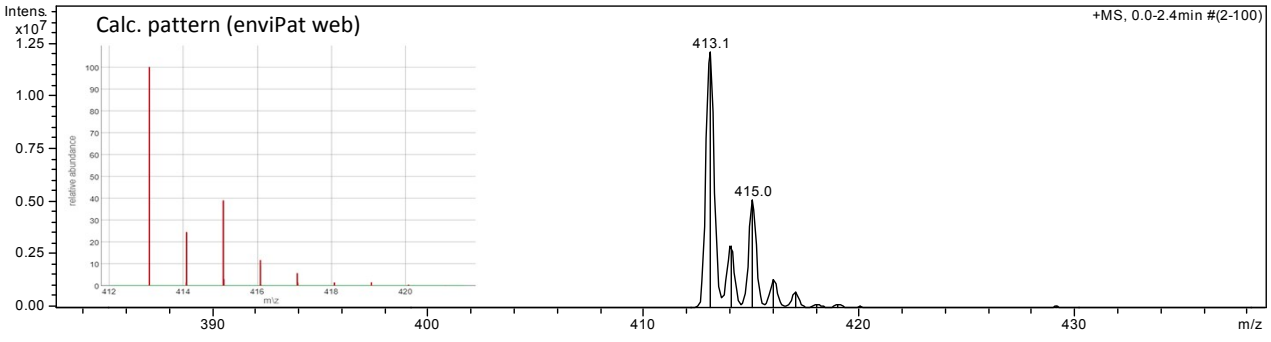

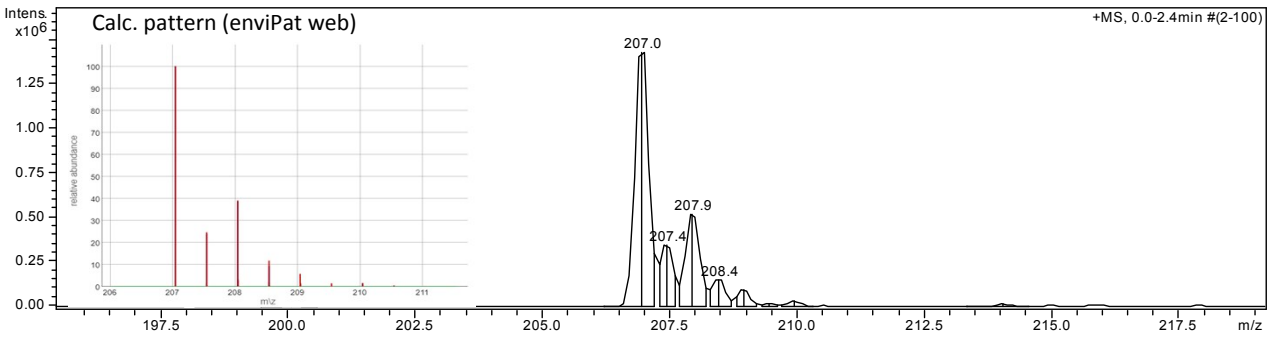

Complex 3c: The final product is a dark green crystal and the yield was 85%.

IR (KBr, cm^{-1}): 3398, 2354, 1645, 1452, 1106, 765, 623.

ESI+ MS (m/z): Calc. for $M^{2+} + Cl^- = C_{22}H_{19}FeN_4OCl$: 446.1, **Found** 446.0.

Elemental Analysis (calc.) $C_{22}H_{19}FeN_4O{*}2ClO_4{*}H_2O$ = C: 42.07%; H: 3.37%; N: 8.92% **Found** = C: 42.47%; H: 3.36%; N: 9.12%.

IR (KBr, cm^{-1})

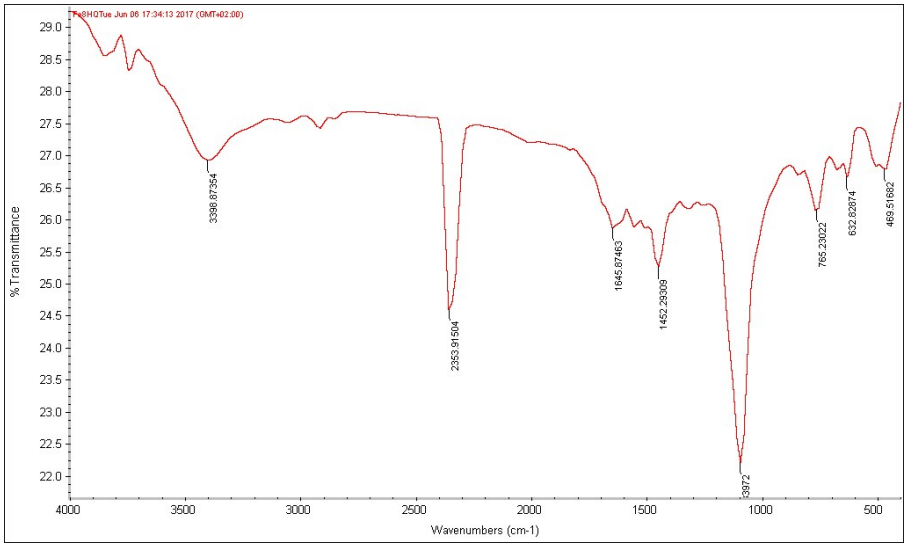

ESI+ MS (m/z)

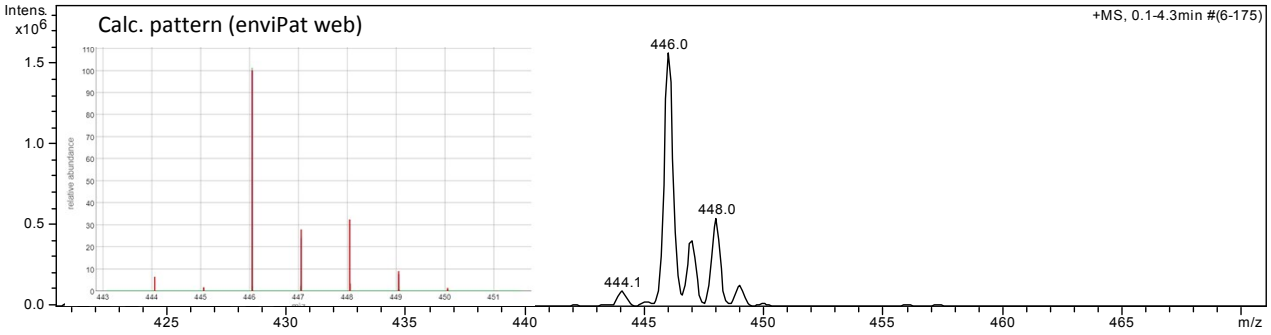

Complex 3d: The final product is a dark yellow crystal and the yield was 87%.

^{1}H NMR (200 MHz, CD_3CN): δ (ppm) = 8.81 (d, 2H, HAr), 8.52 (d, 1H, HAr), 8.12 (dt, 2H, HAr), 7.63 (m, 9H, HAr), 4.47 (d, 4H, CH_2), 4.39 (s, 2H, CH_2).

IR (KBr, cm^{-1}): 3439, 1617, 1447, 1098, 762, 629.

ESI+ MS (m/z): Calc. for $M^+ = C_{22}H_{19}ZnN_4O$: 419.1, **Found** 419.1.

Elemental Analysis (calc.) $C_{22}H_{19}ZnN_4O{*}ClO_4{*}H_2O{*}CH_3CN$ = C: 49.76%; H: 4.18%; N: 12.09% **Found** = C: 49.90%; H: 3.93%; N: 12.41%.

^{1}H NMR (200 MHz, CD_3CN):

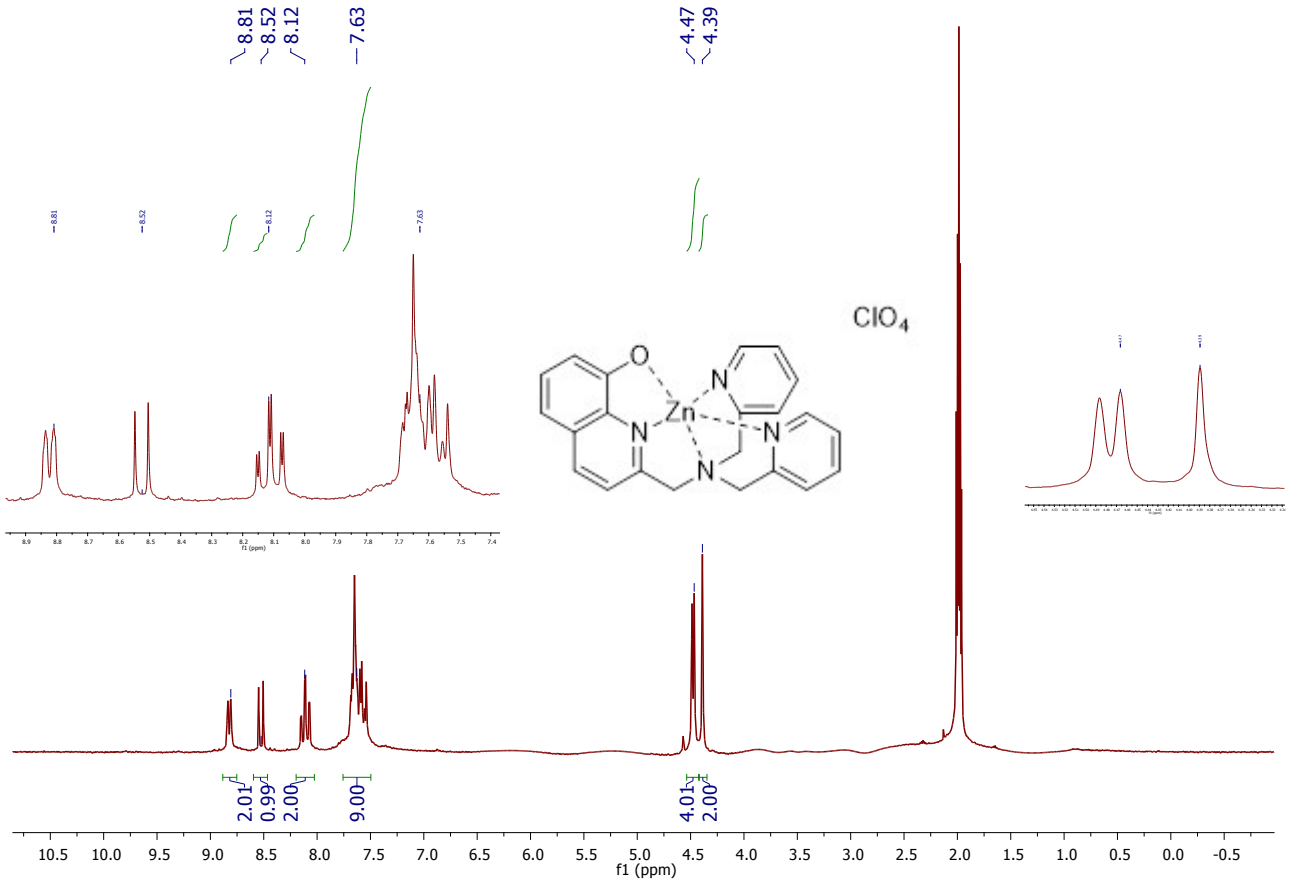

IR (KBr, cm^{-1})

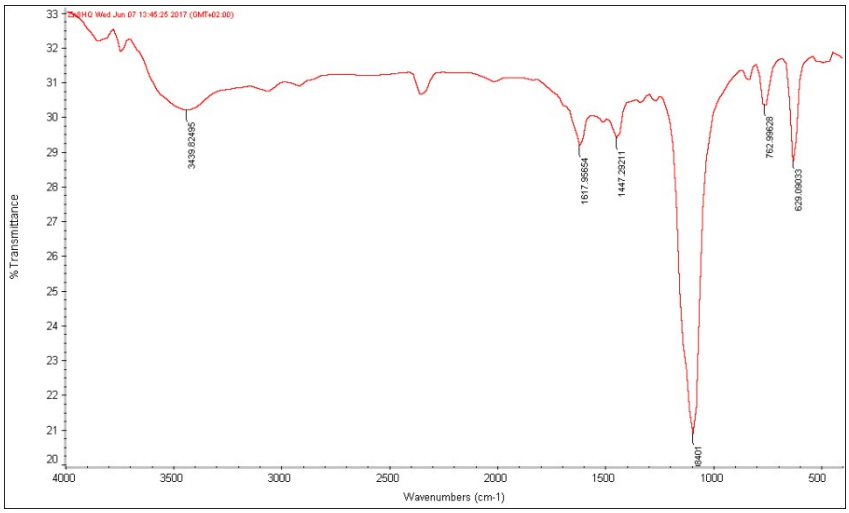
% Transmittance
Wavenumbers (cm-1)
3438.82495
1617.95654
1447.29211
762.98628
629.09033
6401

ESI+ MS (m/z)

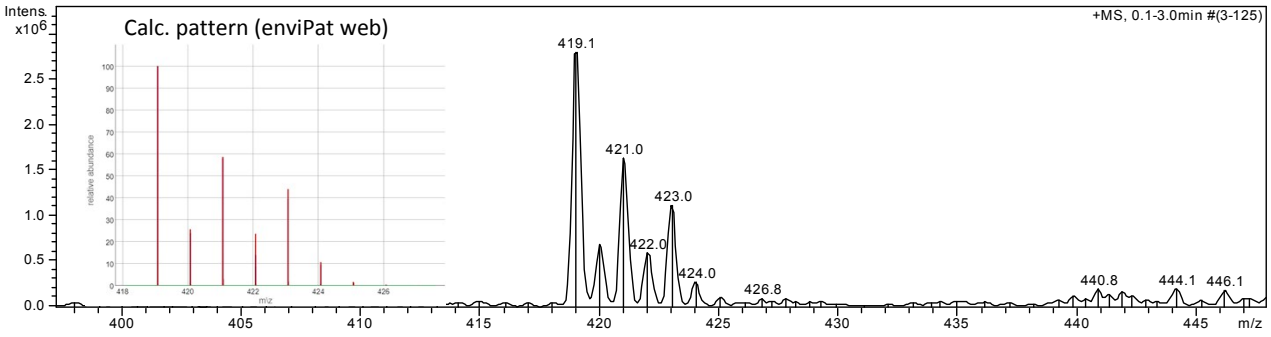
Intens.
x10^6
Calc. pattern (enviPat web)
relative abundance
m/z
+MS, 0.1-3.0min #(3-125)
419.1
421.0
423.0
422.0
424.0
426.8
440.8
444.1
446.1
m/z

Table S1. Relevant crystallographic data obtained from X-ray diffraction on crystals of complexes **3a** and **3c**.

	3a	**3c**
Space Group	I 4_1/a	P -1
Cell Lengths (Å)	a 11.8893(5) b 11.8893(5) c 42.742(2)	a 12.5578(4) b 12.6591(5) c 18.4393(6)
Cell Angles (°)	α 90 β 90 γ 90	α 86.2019(14) β 83.5197(14) γ 68.4545(13)
Cell Volume (Å^3)	6041.81	2708.09
Z, Z'	Z: 8 Z': 0	Z: 2 Z': 0
R factor	4.6	3.93

Table S2. Relevant bond lengths of complex **3a**.

Atom 1	Atom 2	Length (Å)
Co(1)	**N(1)**	1.939
Co(1)	**N(3)**	1.926
Co(1)	**N(3A)**	1.926
Co(1)	**N(2)**	1.734
Co(1)	**O(1)**	1.928
Co(1)	**N(4)**	2.012

Table S3. Relevant bond angles of complex **3a**.

Angle	(°)
N(1)-Co(1)-N(2)	88.24
N(1)-Co(1)-N(3)	83.02
N(1)-Co(1)-N(3A)	86.42
N(1)-Co(1)-N(4)	95.44
N(2)-Co(1)-O(1)	87.64
N(2)-Co(1)-N(3)	89.57
N(2)-Co(1)-N(3A)	91.93
N(3)-Co(1)-O(1)	96.64
N(3)-Co(1)-N(4)	90.13
N(3A)-Co(1)-O(1)	94. 02
N(3A)-Co(1)-N(4)	89.05
N(4)-Co(1)-O(1)	88.68

Table S4. Relevant bond lengths of the **$(3c)_2OH$** dimer.

Atom 1	Atom 2	Length (Å)
Fe(1)	**O(1)**	1.916
Fe(1)	**O(3)**	1.953
Fe(1)	**N(1)**	2.289
Fe(1)	**N(2)**	2.088
Fe(1)	**N(3)**	2.101
Fe(1)	**N(4)**	2.102
Fe(2)	**O(2)**	1.936
Fe(2)	**O(3)**	1.969
Fe(2)	**N(5)**	2.305
Fe(2)	**N(6)**	2.074
Fe(2)	**N(7)**	2.097
Fe(2)	**N(8)**	2.116
Fe(1)	**Fe(2)**	3.710

Table S5. Relevant bond angles of the **$(3c)_2OH$** dimer.

Angle	(°)
N(1)-Fe(1)-N(2)	73.69
N(2)-Fe(1)-O(1)	79.46
O(1)-Fe(1)-O(3)	100.27
N(1)-Fe(1)-O(3)	106.59
N(3)-Fe(1)-O(3)	92.82
N(4)-Fe(1)-O(3)	89.69
N(4)-Fe(1)-N(2)	90.26
N(3)-Fe(1)-N(2)	87.36
N(3)-Fe(1)-O(1)	103.73
N(3)-Fe(1)-N(1)	76.64
N(4)-Fe(1)-N(1)	76.97
N(4)-Fe(1)-O(1)	102.16
Fe(1)-O(3)-Fe(2)	142.07
O(3)-Fe(2)-O(2)	92.02
N(6)-Fe(2)-O(2)	78.75
N(6)-Fe(2)-N(5)	74.26
O(3)-Fe(2)-N(5)	115.02
N(6)-Fe(2)-N(8)	88.79
N(8)-Fe(2)-O(3)	91.77
N(7)-Fe(2)-O(3)	92.63
N(6)-Fe(2)-N(7)	91.42
N(7)-Fe(2)-O(2)	102.90
N(5)-Fe(2)-N(7)	76.14
N(8)-Fe(2)-O(2)	105.51
N(5)-Fe(2)-N(8)	76.10

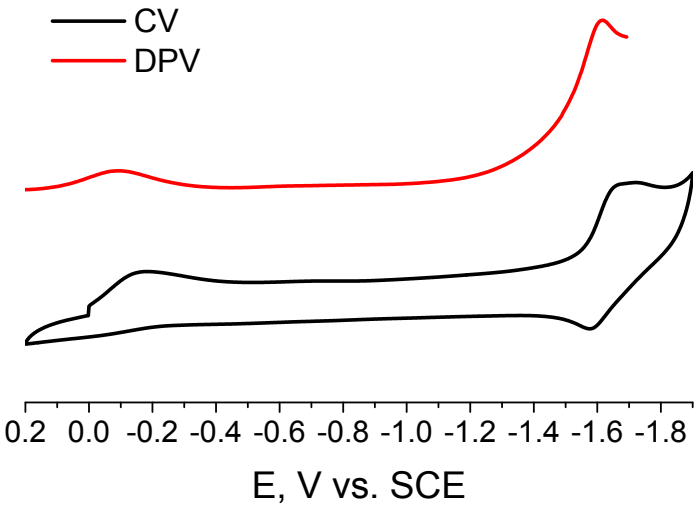

Figure S1. Cyclic voltammetry (CV) and differential pulse voltammetry (DPV) of 1 mM **3a** in acetonitrile solution (0.1 M $TBAPF_6$).

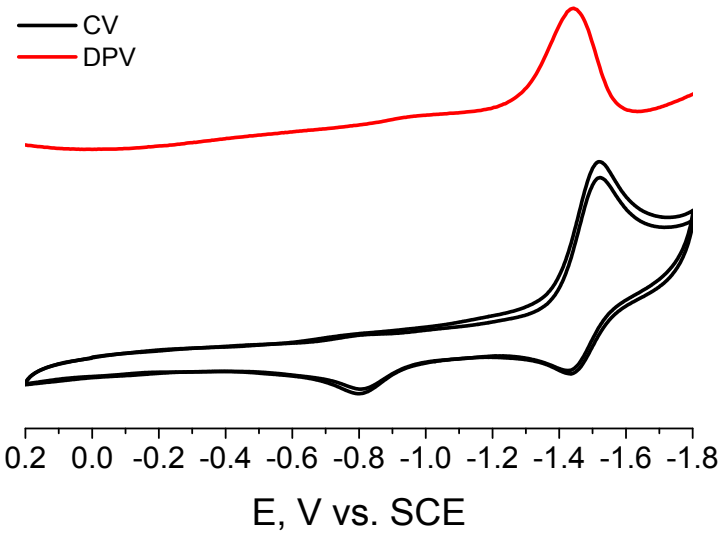

Figure S2. Cyclic voltammetry (CV) and differential pulse voltammetry (DPV) of 1 mM **3b** in acetonitrile solution (0.1 M $TBAPF_6$).

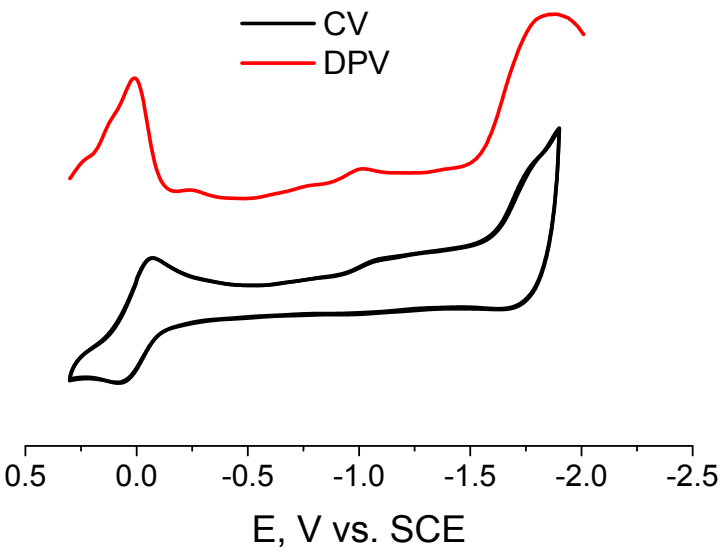

Figure S3. Cyclic voltammetry (CV) and differential pulse voltammetry (DPV) of 1 mM **3c** in acetonitrile solution (0.1 M $TBAPF_6$).

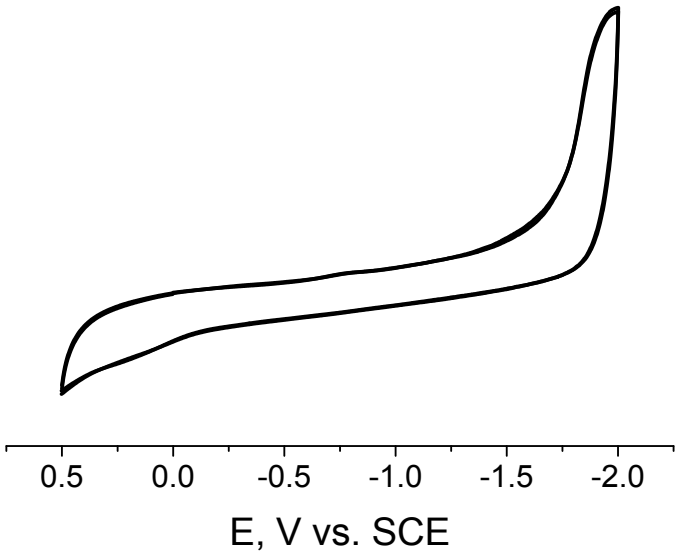

Figure S4. Cyclic voltammetry (CV) of 1 mM **3d** in acetonitrile solution (0.1 M $TBAPF_6$).

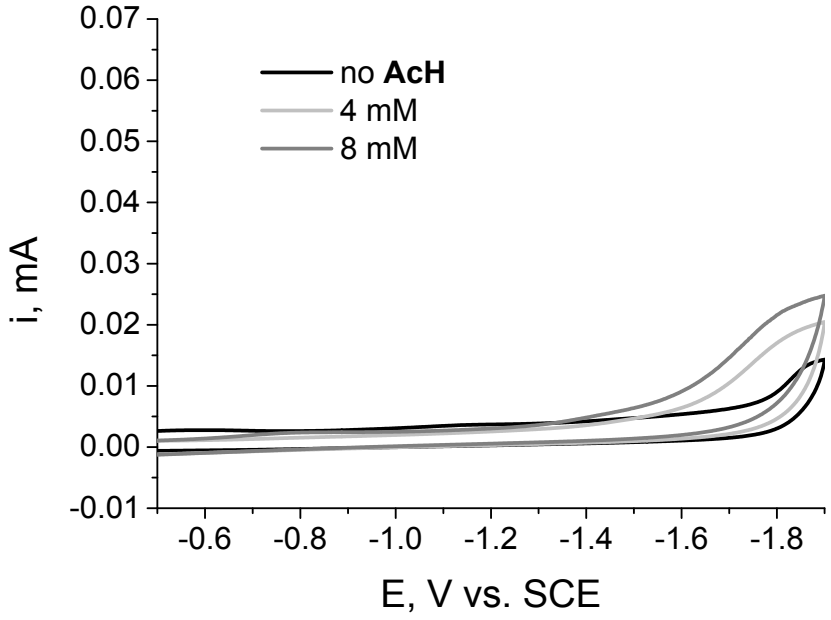

Figure S5. Cyclic voltammetry (CV) of 1 mM **3d** acetonitrile solution (0.1 M $TBAPF_6$) upon addition of 0-8 mM acetic acid.

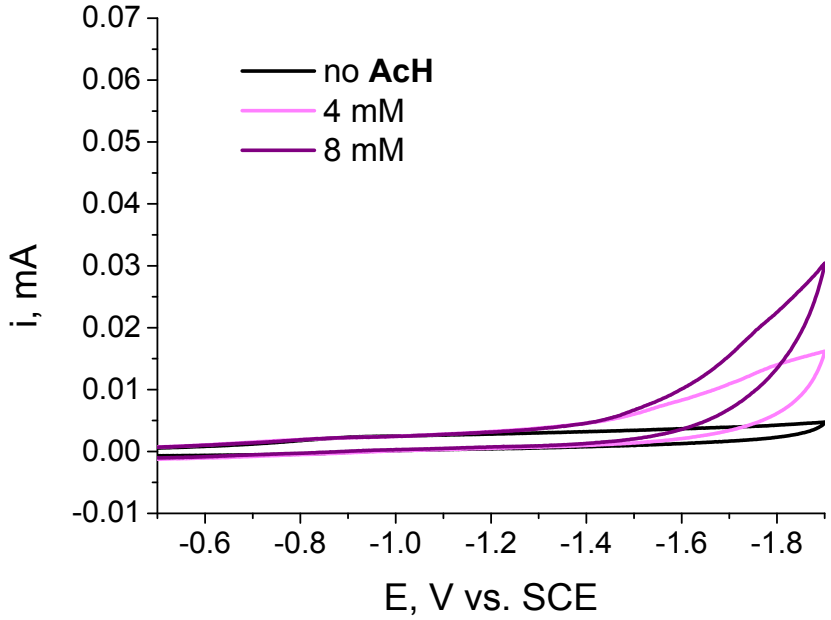

Figure S6. Cyclic voltammetry (CV) of an acetonitrile solution (0.1 M $TBAPF_6$) upon addition of 0-8 mM acetic acid.

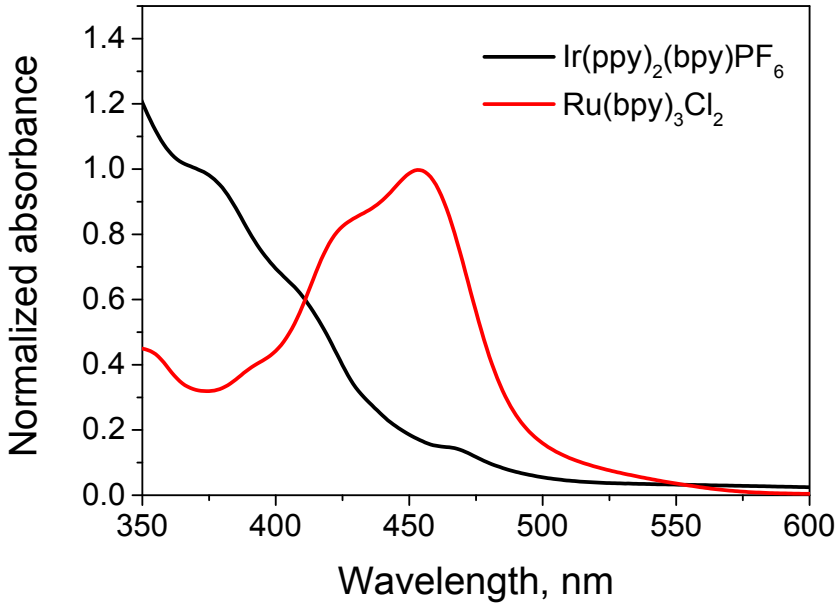

Figure S7. Normalized absorption spectra of $Ir(ppy)_2(bpy)PF_6$ in 45/45/10 acetonitrile/water/TEA mixture and $Ru(bpy)_3Cl_2 \cdot 6H_2O$ in 1 M acetate buffer pH 5.

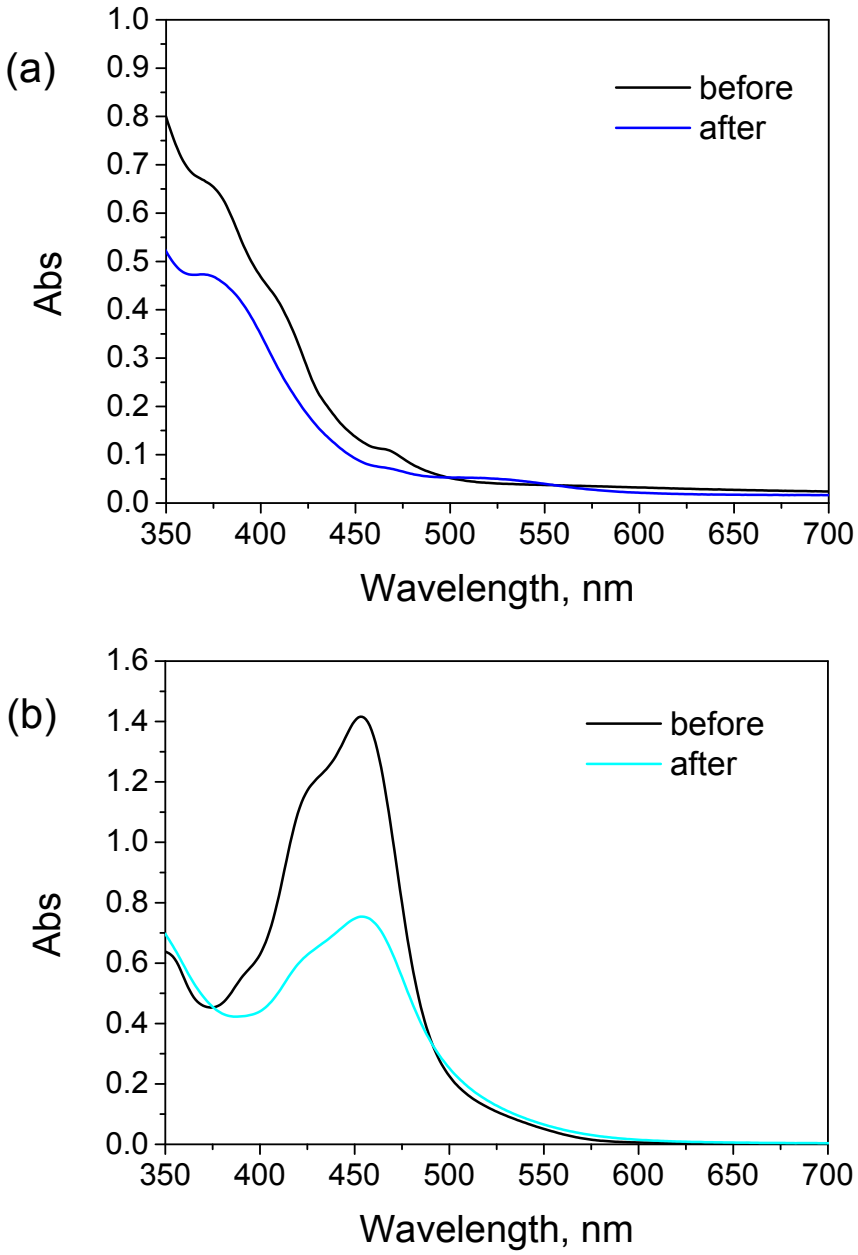

Figure S8. Comparison of absorption spectra before/after 2 h photocatalysis accomplished by the cobalt complex **3a** in the (a) iridium- and (b) ruthenium-based photochemical systems.

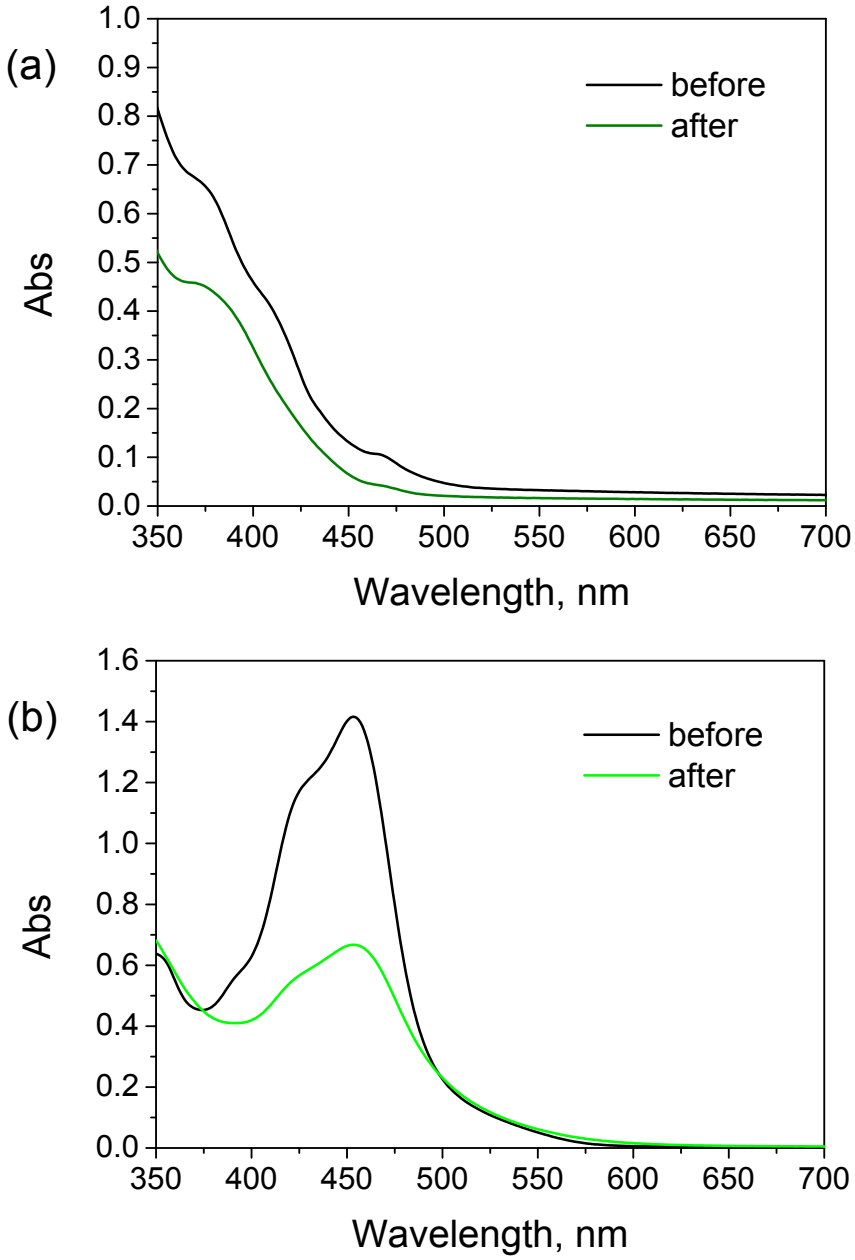

Figure S9. Comparison of absorption spectra before/after 2 h photocatalysis accomplished by the nickel complex **3b** in the (a) iridium- and (b) ruthenium-based photochemical systems.

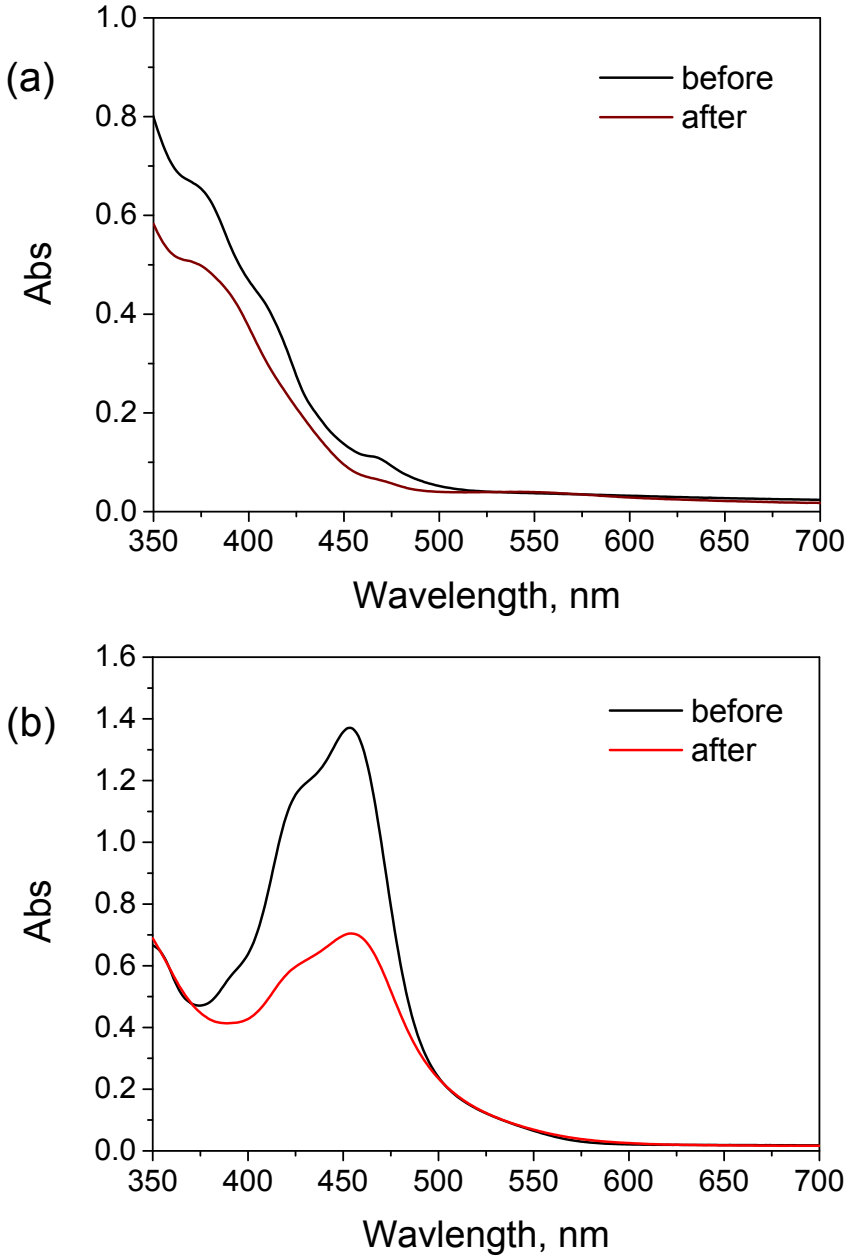

Figure S10. Comparison of absorption spectra before/after 2 h photocatalysis accomplished by the iron complex **3c** in the (a) iridium- and (b) ruthenium-based photochemical systems.

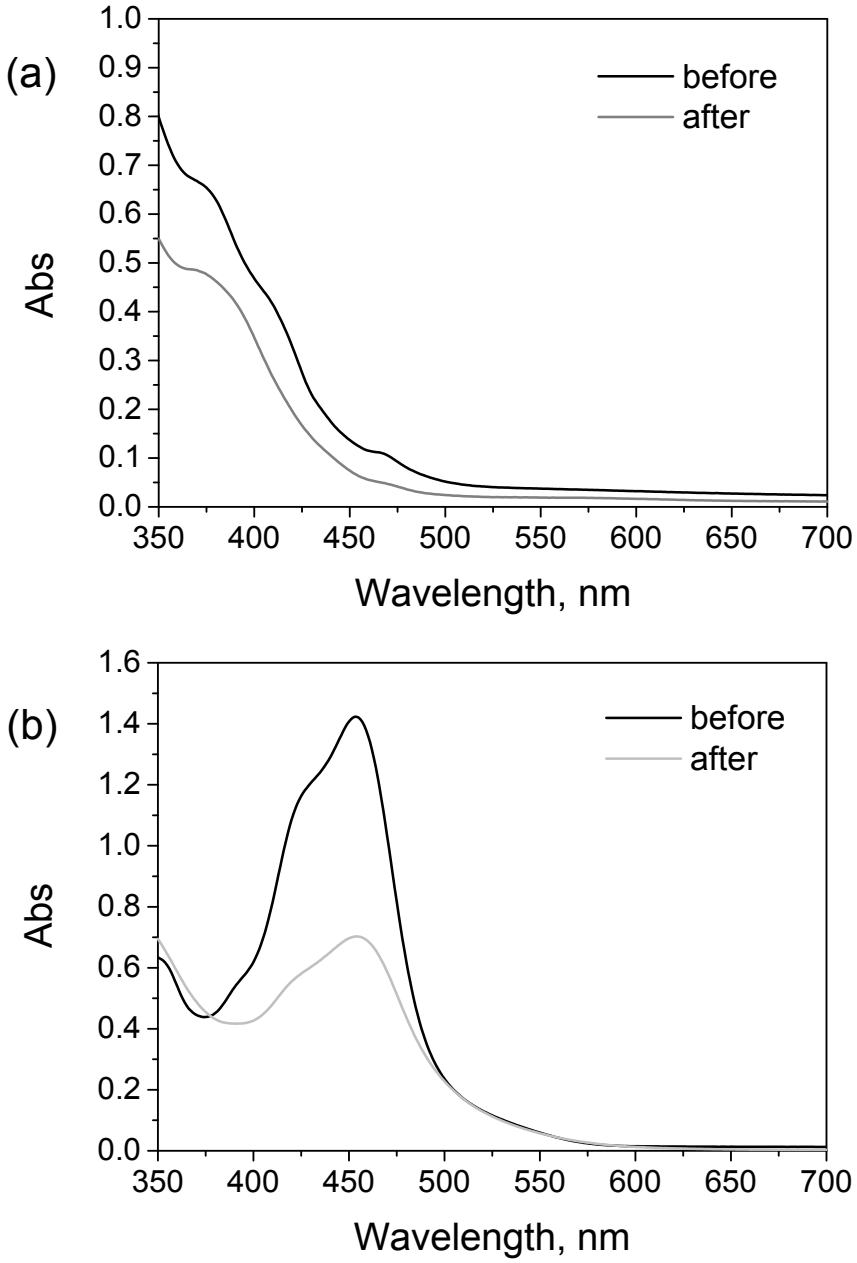

Figure S11. Comparison of absorption spectra before/after 2 h photocatalysis accomplished by the zinc complex **3d** in the (a) iridium- and (b) ruthenium-based photochemical systems.